



# Seismic Effect Analysis of High-Filled Cuter Cover Tunnel Considering the Time-dependent Nature of Fill Soil

Xuhong Shi<sup>1</sup>, Sheng Li<sup>1,\*</sup>, Li Ma<sup>1</sup>, Jiangong Zhang<sup>2</sup>, Lei Cai<sup>3</sup> and Xuefeng Ban<sup>4</sup>

<sup>1</sup>Lanzhou Jiaotong University, School of Civil Engineering, Lanzhou 730070, China

<sup>2</sup>China Seventeen Metallurgical Group Co. Ltd. Maanshan, Anhui, 243000, China

<sup>3</sup>Track Maintenance Department, China Railway Lanzhou Group Co., Ltd., Lanzhou, Gansu, 730030, China

<sup>4</sup>China Railway Construction Group Co., Ltd., Beijing, 100053, China

\*Corresponding author's e-mail: ligwin@126.com

**Abstract.** In order to investigate the seismic effect analysis of High-Filled Cuter Cover Tunnel based on equal load reduction rate and considering the timeliness of filling, three load-reducing materials, namely, EPS board, low-pressure solid soil and rubber granular improved soil, are selected, and the effects of the differences in load-reducing materials on the soil pressure around the caves and the safety of the lining are analyzed under the effect of earthquakes, using a combination of experiments and numerical simulations. The results show that: under seismic action, the average vertical dynamic soil pressure on the left side of the cave roof is 1.12~1.05~1.02 times of the static loaded soil pressure, and the dynamic soil pressure on the right side is 1.02~1.01~1 times of that on the left side; the horizontal dynamic soil pressure on the left and right sides of the cave shows a trend of "this is the opposite of the other", and the average horizontal dynamic soil pressure on the left side of the cave is 0.5~2 times of that on the right side. The average horizontal dynamic soil pressure on the left side (right side) of the hole is 0.63~0.88~1.03 times (1.95~1.32~1.08 times) of the static load soil pressure. The distribution of structural safety coefficient tends to be symmetrical from asymmetric in order, and the smallest part of the safety coefficient is transferred from the arch top to the right side wall. When seismic design is carried out in High-Filled Cuter Cover Tunnel, attention should be paid to the safety performance of the lining structure arch top and right side wall.

**Keywords:** High-Filled Cuter Cover Tunnel; equal reduction rate; earthquake; creep; factor of safety.

## 1 Introduction

As a new type of underground structure, High-Filled Cuter Cover Tunnel is now widely used in the construction of Northwest Railway, which not only relieves the urban land, but also increases the urban land area. However, the creep performance of the fill and

© The Author(s) 2024

P. Xiang et al. (eds.), *Proceedings of the 2023 5th International Conference on Hydraulic, Civil and Construction Engineering (HCCE 2023)*, Atlantis Highlights in Engineering 26,

[https://doi.org/10.2991/978-94-6463-398-6\\_8](https://doi.org/10.2991/978-94-6463-398-6_8)

load shedding material makes the soil stress redistributed and the structural stress performance changed. And the Northwest region frequent earthquakes, so in the creep stage, under the action of earthquakes, soil pressure changes within the soil body and structural safety performance research is of great significance.

Numerous scholars have done research on the stress performance of High-Filled Cuter Cover Tunnel under the action of fill creep. Liu Xuekui<sup>[1]</sup> carried out long-term numerical simulation of High-Filled Cuter Cover Tunnel by means of finite difference software, and analyzed the development of soil arch morphology of the fill soil at the top of the caves and the timeliness of the structural response. In the literature<sup>[2-3]</sup> Jia Nie Yuchi<sup>[4-5]</sup> the creep characteristics of backfilled loess were considered and the time-dependent changes in soil displacement, soil pressure and structural internal force within the high fill range were analyzed. Gao Qi<sup>[6]</sup> Using a combination of model test and numerical simulation, analyze the stress redistribution law of bridge and culvert-soil body and the long-term stress characteristics of high-fill box culvert, put forward the mechanical model of culvert-soil system, and deduce the long-term soil pressure calculation method. Hu Shijin et al.<sup>[7-8]</sup> analyzed the internal force distribution of lining based on numerical simulation method, and assessed the safety of secondary lining according to the specification requirements. Ou Xiangping et al.<sup>[9]</sup> The safety performance of the tunnel was analyzed based on the creep of the soil with a safety factor.

In addition, the change of fill soil pressure under seismic action is also bound to cause the change of structural safety. Yong<sup>[10]</sup> used finite element software to explore the influence of tunnel buried depth, stiffness, wave incident angle and other factors on the seismic response of the tunnel. Liu<sup>[11]</sup> studied the dynamic response of the tunnel with seismic isolation measures after the incident SV wave. You Zhigang<sup>[12-13]</sup> Based on numerical simulation, the soil arch morphology of the soil body and the dynamic response of lining structure at the cave roof under different seismic waves with different accelerations were investigated. Guo Jun et al.<sup>[14]</sup> Seismic calculation of tunnel open hole structure using finite difference software was carried out, and the internal force response law of the lining structure was derived, and the safety of the lining structure was analyzed and studied. Zhang Zhaotong et al.<sup>[15]</sup> Adopted the exogenous fluctuation input method with viscoelastic boundary combined with equivalent load to comparatively analyze the influence of different waves on the seismic response of tunnel lining structure.

It can be seen that the current study mainly focuses on the long-term change of fill soil pressure, displacement and structural internal force under the action of fill creep in High-Filled Cuter Cover Tunnel, but there are fewer researches on the change of soil pressure on the roof of the cave and the safety of lining structure under the action of creep stage and earthquake. In this paper, three different load shedding materials are taken, and under the condition of the same load shedding rate at the top of the hole, the creep stage, and the seismic action, the soil pressure at the top and side of the hole and the safety performance of the structure are studied.

## 2 Creep test

### 2.1 Pilot program

The materials selected for the test are loess, rubber particles and EPS board. The loess was taken from Lanzhou New District, Gansu Province, and the indoor geotechnical test was carried out according to the Standard for Geotechnical Test Methods (GB/T 50123-2019), and the basic mechanical parameters of the loess are shown in Table 1 below.

**Table 1.** Basic mechanical parameters of loess.

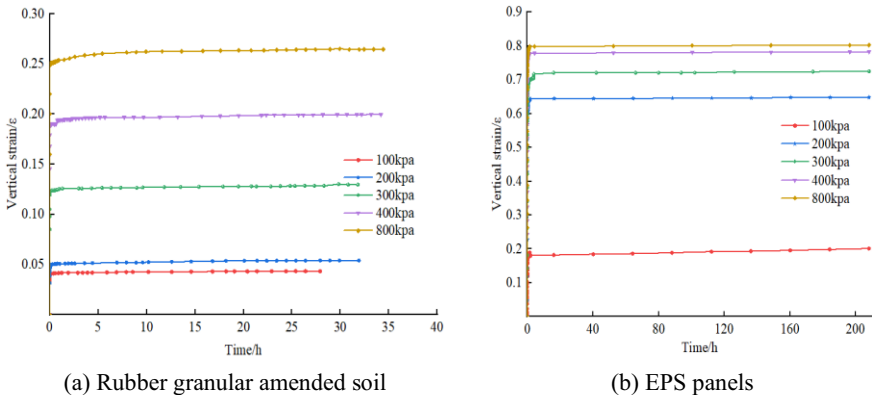
Liquid Limit $W_L$ (%)	Plastic limit $W_P$ (%)	Plasticity Index $I_P$	Optimum moisture con- tent $W_O$ (%)	Maximum dry den- sity $P_{dmax}$ ( $g \cdot cm^{-3}$ )
18.53	8.75	9.78	10.6	2.15

The test specimens were rubber granule amended soil, EPS board and 85% compaction loess and 95% compaction loess. The rubber granule amended soil is used 30% dosage, 30% dosage is the rubber granule mass accounted for 30% of the total mass of rubber granule, loess and water under the optimal moisture content. density of EPS plate is  $30kg/m^3$ .

Uniaxial consolidation test is now used to study the creep characteristics of the material, the instrument is used uniaxial consolidation instrument, select the height of 2cm, the area of  $30cm^2$  cylindrical ring knife specimen, using separate loading, loading pressure were 100, 200, 300, 400, 800 kPa, real-time recording of the percentage meter readings during the loading process, and deformation is less than  $0.005mm/d$  is set as a stable creep State.

### 2.2 Test results and analysis

Figure 1 shows the vertical strain-time curves obtained from creep tests of different materials.



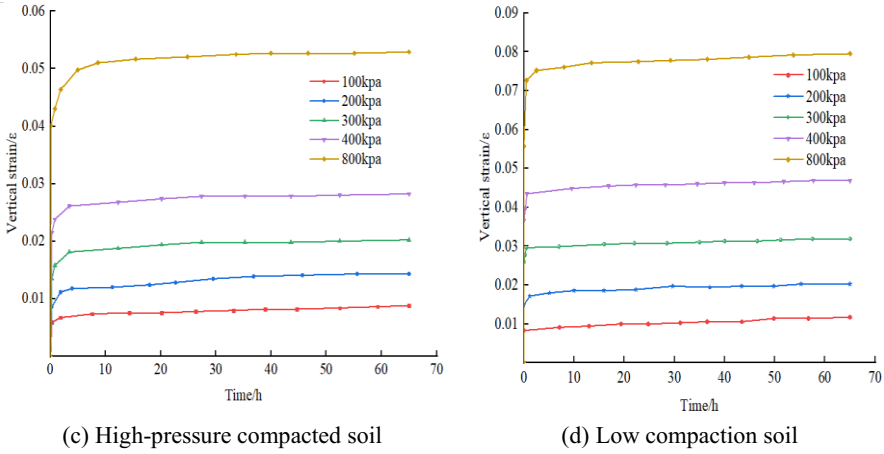


**Fig. 1.** Vertical strain-time curves for different materials.

As can be seen from Figure 1: (1) under all levels of loading, there is a significant transient deformation of the specimen at the beginning of loading, and then enters the initial creep stage, the deformation rate gradually becomes smaller, almost 0, and enters the stable creep stage. (2) With the increase of loading pressure, the initial creep stage to the stable creep stage takes longer, and the stage of creep deformation is greater. (3) Under the same loading, the size of vertical strain: EPS plate > rubber granule modified soil > low pressure solid soil > high pressure solid soil.

### 2.3 Burgers model validation and obtaining parameters

The Burgers model can well describe the three stages of instantaneous deformation, initial creep and stable creep of materials, and can be widely used to describe the creep behavior of materials such as soil, EPS panels and improved soils etc. The Burgers model consists of a combination of elemental bodies Maxwell body and Kelvin body, and the creep equation of the model is:

$$\varepsilon(t) = \frac{\sigma_0}{E_M} + \frac{\sigma_0}{\eta_M} + \frac{\sigma_0}{E_K} [1 - \exp(-\frac{\sigma_0}{\eta_K})] \quad (1)$$

The Burgers equation was chosen to fit the strain-time curve to the rubber granular amended soil as an example, as shown in Figure 2.

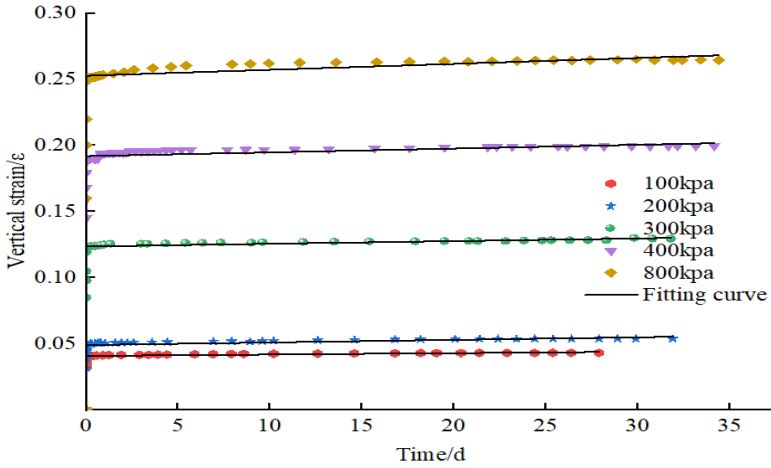


**Fig. 2.** Comparison of test data of rubber granule-amended soil with Burgers' fitted curve.

As can be seen from the figure, the Burgers equation has a high degree of overlap with the test data, and the fitting accuracy reaches more than 0.95, which indicates that the Burgers model can well describe the creep effect of the rubber granular amended soil. The strain time curves of the four specimens were fitted using origin software to obtain the relevant parameters of the Burgers equation. It is shown in table 2~5 below.

**Table 2.** Parameters of Burgers model for soil mixed with 30% dosed rubber particles.

$\sigma$ (kPa)	$E_M$ (MPa)	$E_K$ (MPa)	$\eta_M$ (MPa*h)	$\eta_K$ (MPa*h)
100	221.23	2.5	952.38	0.0009
200	203.25	4.15	1025.64	0.0025
300	119.04	2.47	1497.99	0.0013
400	135.59	2.11	1408.45	0.0009
800	253.96	3.2	1785.71	0.0018

**Table 3.** Parameters of Burgers model for EPS plate.

$\sigma$ (kPa)	$E_M$ (MPa)	$E_K$ (MPa)	$\eta_M$ (MPa*h)	$\eta_K$ (MPa*h)
100	0.39	0.0056	9.86	0.0007
200	0.99	0.0027	23.7	0.00003
300	1.91	0.0036	53.38	0.00002
400	3.31	0.0049	55.14	0.00001
800	4.25	0.0052	58.15	0.00001

**Table 4.** Parameters of Burgers model for high pressure solid soil.

$\sigma$ (kPa)	$E_M$ (MPa)	$E_K$ (MPa)	$\eta_M$ (MPa*h)	$\eta_K$ (MPa*h)
100	18.6	286.87	2221.09	686.37
200	26.62	122.25	4079.17	70.57
300	23.25	78.64	5025.36	48.52
400	19.6	58.73	6297.69	23.61
800	17.79	117.8	18399	32.6

**Table 5.** Parameters of Burgers model for low-pressure solid soil.

$\sigma$ (kPa)	$E_M$ (MPa)	$E_K$ (MPa)	$\eta_M$ (MPa*h)	$\eta_K$ (MPa*h)
100	12.44	80.7	2843.78	234.98
200	13.09	102.8	4551.93	24.75
300	12.52	92.65	6524.23	28.65
400	11.42	87.91	7639.23	32.78
800	11.56	78.05	20771.3	10.33

### 3 Numerical simulation

#### 3.1 Modeling

In order to study the seismic effect analysis of High-Filled Cutter Cover Tunnel under the condition of equal load-shedding rate, considering the time-dependent nature of the fill. Three working conditions are established with EPS board, rubber granular modified soil and low pressure solid soil as load shedding materials and high pressure solid soil as fill soil. As shown in Table 6 below.

**Table 6.** Classification of working conditions.

Load-shedding material landfill	EPS board	low-pressure soil	Rubber granule soil mix
Compacted earth	H1	H2	H3

The model in the paper is modeled by finite difference software, the model boundary size is 96m<sup>[16]</sup>, the foundation thickness is 35m, the slope gradient is 70°, the concrete columns with the same height as the top of the hole are set up on the side of the hole, a certain thickness of load reducing material is set up within the width of the hole at the top of the hole, and the rest of the location is filled with high pressure solid soil, the high pressure solid soil is filled by layer filling, and the filling thickness of each layer is 5m. After the model is established, static constraints are applied to the model boundary. Static constraints. After the static calculation is completed, open the dynamics plate, input the classical Kobe wave, select the peak acceleration of ground vibration as

0.3g, and adjust the free-field boundary conditions required by the model. This is shown in Figure 3 below.

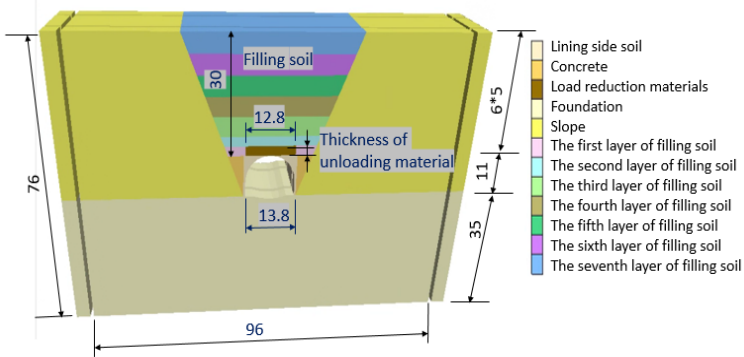


Fig. 3. Model diagram of High-Filled Cuter Cover Tunnel.

In addition, the earth pressure on the roof and sides of the cave and the safety performance of each part of the lining are analyzed, and measuring points are set up in the corresponding positions of the model, as shown in Figure 4. Among them, the A-A section measuring point monitors the vertical earth pressure on the roof of the cave, the B-B section (C-C) measuring point monitors the horizontal earth pressure on the left (right) side of the open hole, and the lining structure measuring point is used to monitor the axial force and bending moment at each point.

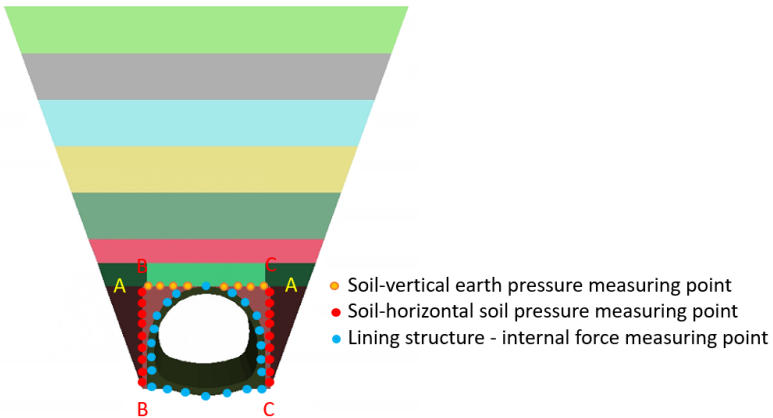


Fig. 4. Monitoring points of soil pressure and lining internal force at the roof and sides of the hole.

### 3.2 Selection of material parameters

This paper is divided into three parts to analyze the soil pressure and structural safety of the perimeter of the hole under seismic action at different times (0, 1 and 10 years)

after the completion of the fill, respectively. When the filling is completed, the lining, slope, foundation and concrete column are given elastic-plastic constitutive model, the parameters are derived from the research results of the literature [17], the parameters of load shedding material and high pressure solid soil are based on geotechnical test, the material parameters are shown in the following table 7. the creep parameters of the material during the creep stage of the load shedding material and the filling soil are shown in the above table 7.

**Table 7.** Numerical model parameters.

makings	Modulus of elasticity (kPa)	Poisson's ratio	Cohe-sion (kPa)	Angle of inter-nal friction (°)	Density (g*cm <sup>-3</sup> )
slope	4.19e6	0.2	75	26	2.0
foundations	2.17e7	0.2	-	-	2.5
Lining	3.25e7	0.2	-	-	2.5
concrete column	3.00e7	0.2	-	-	2.5
low-pressure soil	5.40e3	0.3	31	28.24	1.77
compacted earth	1.24e4	0.3	77	31.53	1.97
30% rubber gran-ule soil mix	2.40e3	0.3	27.5	18.7	1.92

#### 4 Determination of equal load-shedding rates

The laying of load reducing material on the roof of the cave makes the soil arch formed on the roof of the cave, which reduces the soil pressure on the roof of the cave. However, due to the creep performance of the fill, it makes the effect of load reduction on the roof of the cave changed. In this paper, the load shedding rate is utilized to describe the change of soil pressure on the roof of the cave, and the load shedding rate formula is shown below:

$$\varepsilon = 1 - \frac{P_a}{P} \quad (2)$$

Where:  $\varepsilon$  is the load reduction rate,  $P_a$  and  $P$  are the soil pressure at the top of the hole and the theoretical soil pressure at the top of the hole, respectively.

In order to make the soil pressure at the roof of the cave reach the same or similar load reduction rate under different load reduction measures, i.e. equal load reduction rate. Now more sub-cases are established to control the load reduction rate under different load reduction measures by adjusting the thickness of load reduction materials. As shown in Table 8 below.



**Table 8.** Determination of equal load reduction rates.

	Working condition H1					Working condition H2					Working condition H3				
working condition	1	2	3	4	5	1	2	3	4	5	1	2	3	4	5
Thickness of load shedding material/m	0.2	0.25	0.5	1	1.5	5	6	8	10	12	1.5	2	2.5	3	3.5
Thickness of filling soil at the top of the hole/m	29.8	29.75	29.5	29	28.5	25	24	22	20	18	28.5	28	27.5	27	26.5

Calculated by the above formula, the load shedding rate under each sub-condition is determined, and the load shedding rate curve is plotted, as shown in Figure 5 below. As can be seen from Figure 5, the load reduction effect is significant with increasing the thickness of load reducing material under H1 and H3 conditions. And the maximum load shedding rate under H2 condition is 30%. Therefore, in order to optimize the load shedding effect under the three conditions, the equal load shedding rate of 30% is selected for the H1-2, H2-4 and H3-3 conditions, respectively.

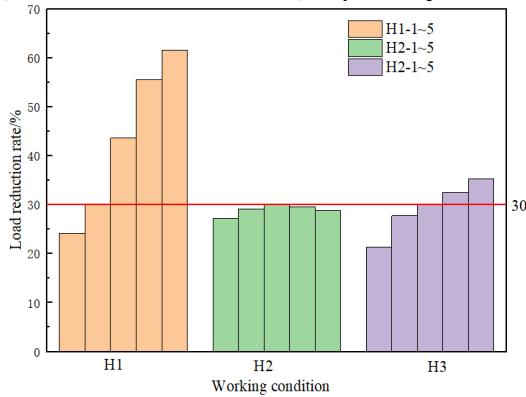


**Fig. 5.** Determination of equal load shedding rate.

## 5 Research on seismic effects

### 5.1 Vertical earth pressure

In order to analyze the effect of earthquake on the dynamic performance of High-Filled Cutter Cover Tunnel at different times after the completion of filling, this paper analyzes the following scenarios: ① earthquake immediately after the completion of filling; ② earthquake occurs 1 year after the completion of filling; ③ earthquake occurs 10 years after the completion of filling. During the earthquake, the peak vertical dynamic soil pressure of the vault occurs, and in order to clarify the difference between the peak

dynamic soil pressure of A-A section and the static load soil pressure, a comparative analysis of the two is carried out, as shown in Figure 6 below.

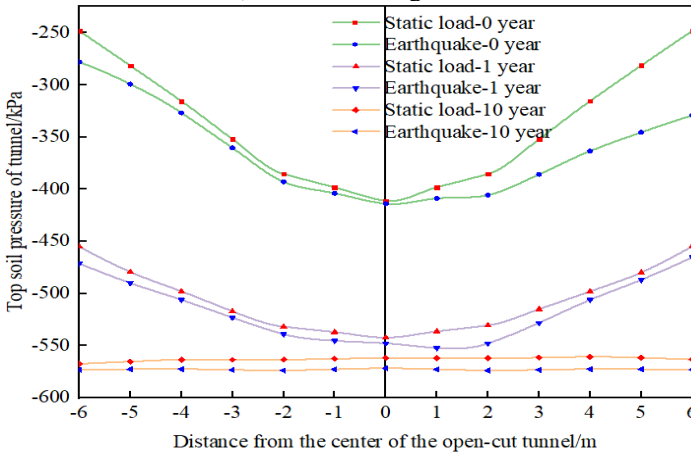


Fig. 6. Vertical earth pressure diagram for H3-3 conditions.

Figure 6 shows the distribution of vertical earth pressure of A-A section under static load-earthquake comparison. Under static load, the vertical earth pressure of A-A section was U-shaped symmetrical distribution, with the creep of the fill, the vertical earth pressure of A-A section increased to the size of the theoretical earth pressure; under seismic action, the distribution of vertical earth pressure is similar to the static earth pressure, but the earth pressure value has increased and the increase of the vertical earth pressure on the left side of the roof of the cave is smaller than the right side. Equivalent load method<sup>[18]</sup> Calculated by "equivalent load method<sup>[18]</sup>", the average vertical earth pressure on the left side (right side) of the cave roof under seismic action is 1.12~1.05~1.02 times (1.15~1.06~1.02 times) of that under static loading at different time periods after the completion of filling. It can be seen that the increase of vertical earth pressure on both sides of the roof of the cave is getting smaller in different time periods after the completion of filling, and the change of earth pressure under seismic action is the largest in 0 years after the completion of filling.

In order to better describe the change of earth pressure under seismic action, the earth pressure amplification factor  $\alpha$  is defined and is shown in Equation 2 below.

$$\alpha = \frac{P_a}{p} \tag{3}$$

Where:  $p_a$  is the vertical earth pressure under seismic action,  $p$  is the vertical earth pressure under static load action

Table 9 shows the comparison of vertical mean earth pressures in section A-A under static load-earthquake.

**Table 9.** Amplification factor of vertical earth pressure under seismic action.

	0 year after completion of fill		1 year after completion of fill		10 years after completion of fill	
	Left side of the cave roof	Right side of the cave roof	Left side of the cave roof	Right side of the cave roof	Left side of the cave roof	Right side of the cave roof
H1-2	1.119	1.145	1.048	1.061	1.025	1.027
H2-4	1.014	1.134	1.012	1.019	1.004	1.003
H3-3	1.010	1.133	1.017	1.021	1.006	1.010

From Table 9, it can be seen that under the effect of earthquake, the earth pressure amplification factor are greater than 1, the overall increase in earth pressure at the roof of the cave, and the increase in earth pressure; 0 years after the completion of the filling > 1 year after the completion of the filling > 10 years after the completion of the filling. And the increase of earth pressure on the left side is smaller than that on the right side, showing the trend of tilting to one side. The amplification coefficients of vertical earth pressure at each stage after the completion of filling: H1-2 condition > H3-3 condition > H2-4 condition.

### 5.2 Horizontal earth pressure

Figure 7 shows the distribution of horizontal earth pressures in sections B-B and C-C on the hole side.

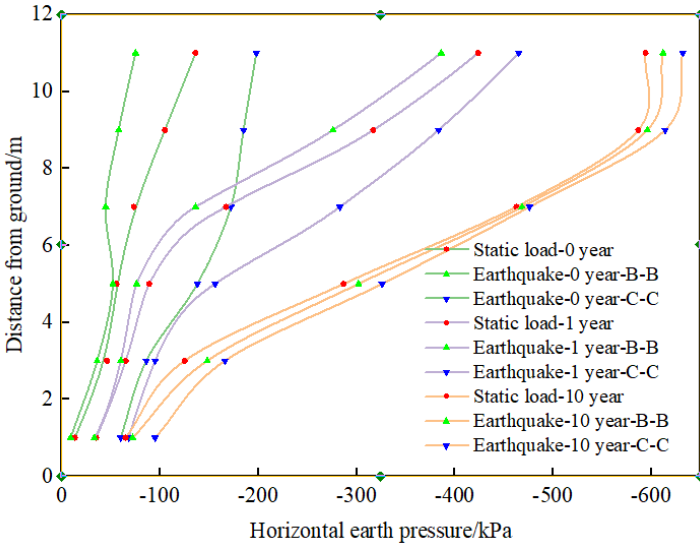


**Fig. 7.** Horizontal earth pressure distribution in sections B-B and C-C.

As can be seen from Fig. 7; under static load, the horizontal earth pressure increases with the increase of distance from the foundation, and with the creep of the filling soil, the earth pressure gradually increases, especially from the foundation more than 5m above the change is obvious; under seismic action, the distribution of the horizontal dynamic earth pressure is similar to the static earth pressure, but the horizontal dynamic earth pressure of the B-B cross-section in the completion of the filling of the 0, 1 year is less than the static earth pressure, and the completion of the filling of the 10-year is greater than the static earth pressure. C-C cross-section horizontal dynamic soil pressure is greater than the static load soil pressure after the completion of the fill, and the average horizontal dynamic soil pressure of the B-B cross-section (C-C) under seismic action is 0.63~0.88~1.03 times (1.95~1.32~1.08 times) of that under static load action. It can be seen that the earthquake occurred in 0 and 1 year after the completion of filling, the horizontal earth pressure on the left and right sides of the open hole showed the trend of "both sides increase", and the magnitude of the change was larger in 0 year, and the magnitude of the change was smaller in 1 year. When an earthquake occurs in 10 years after the completion of filling, the horizontal earth pressure on the left and right sides of the open hole has a small increase.

**Table 10.** Amplification factor of horizontal soil pressure in C-C section under seismic action.

	0 years of fill completion	1 year after completion of fill	10 years after completion of fill
H1-2	1.955	1.32	1.08
H2-4	1.146	1.023	1.016
H3-3	1.187	1.029	1.024

Table 10 is the amplification coefficient of horizontal earth pressure on C-C section under earthquake action. From table 7, it can be seen that the amplification coefficient of horizontal earth pressure on section decreases in turn under 0,1 and 10 years of filling completion. The amplification coefficient of horizontal earth pressure is : H1-2 working condition > H3-3 working condition > H2-4 working condition when the filling is completed for 0, 1 and 10 years. It can be seen that the H2-4 case has good seismic isolation performance.

### 5.3 Lining safety characteristics

The lining structure is made of C35 reinforced concrete with a thickness of 1.5 m. The main reinforcement is HRB400  $\Phi$  32 mm with a spacing of 125 mm and a protective layer thickness of 60 mm, and the hoop reinforcement is HPB400  $\Phi$  20 mm. Based on the "Railway Tunnel Design Specification", the effect of the earthquakes on the structural safety of the filling completion of 0, 1 and 10 years is analyzed.

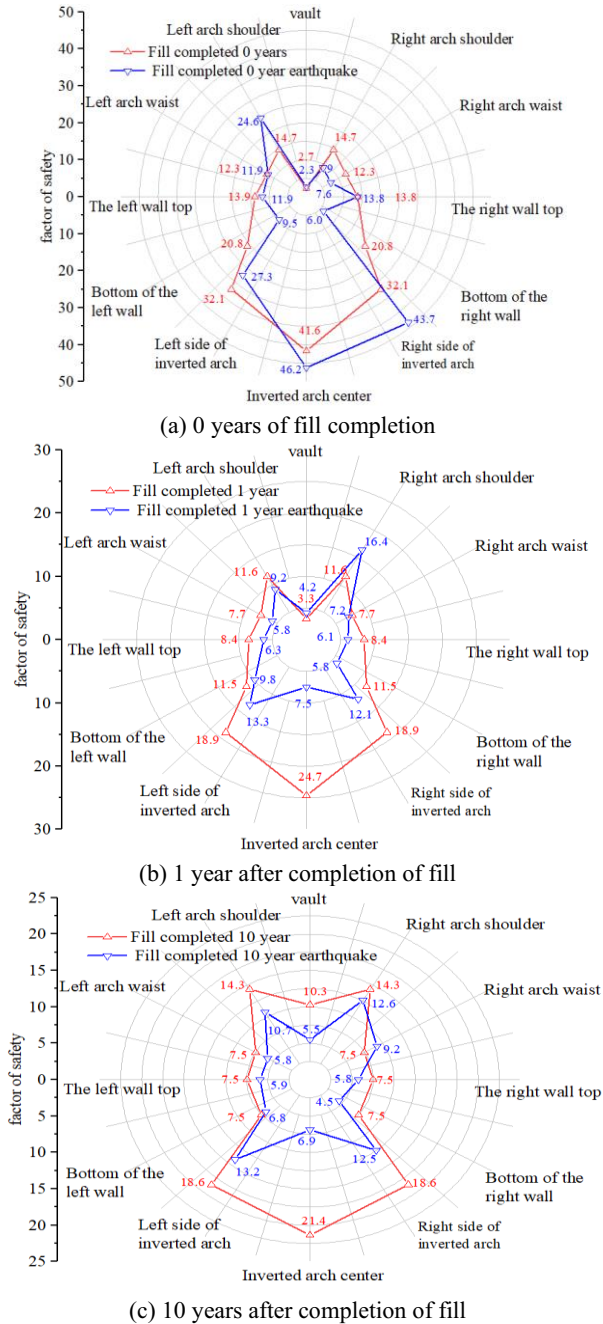
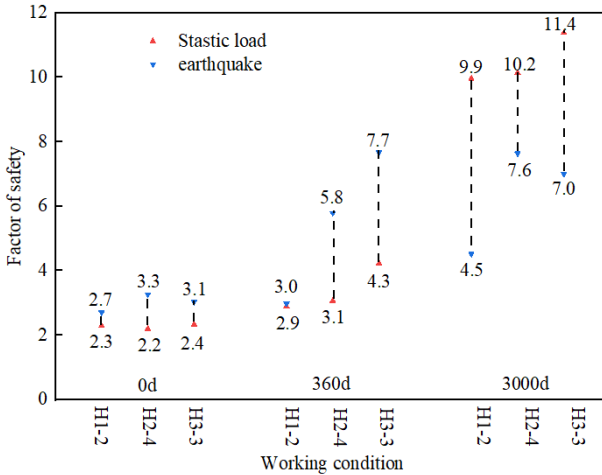


Fig. 8. Distribution of safety coefficients under static load-earthquake action for H3-3 working conditions.



**Fig. 9.** Comparison of the minimum safety factor for each operating condition.

As can be seen in Figures 8 and 9:

(1) In 0 years after the completion of filling, the safety coefficient of both left and right sides of the lining under static load is symmetrically distributed and the safety coefficient of the arch top to the superelevation arch is gradually increasing, and the safety coefficient of the arch top part is the smallest, which is 2.3; under the seismic action, the safety coefficient of the lining on both left and right sides is asymmetrically distributed, and the bottom of the right and left sidewalls safety coefficient is decreasing, and the safety coefficient of the left arch shoulder is increasing from 14.7 to 24.6, and the safety coefficient of the right arch shoulder to the right wall Decrease. This may be because the horizontal soil pressure on the right side of the lining increased greatly, which reduced the safety of the right side of the lining.

(2) 1 year after the completion of filling, the coefficient of safety of all parts of the lining structure under seismic action showed a significant decline, the center of the superelevation arch coefficient of safety decreased the most, from 24.6 to 7.5, and the left and right sides gradually tended to be symmetrical, but there was a significant increase in the right shoulder of the arch, from 11.5 to 16.4. 10 years after the completion of filling, the safety coefficient of the arch top, the shoulder and the superelevation arch parts decreased a lot, and the rest of the parts of the change is smaller, but the bottom of the right wall changed significantly, but the bottom of the right wall was the smallest. In 10 years after the completion of the filling, the safety coefficient of the top of the arch, the arch shoulder and the elevated arch decreased a lot, and the change of the rest of the parts was small, but the change of the safety coefficient of the bottom of the right wall was more obvious, and the safety coefficient of the bottom of the right wall was the smallest, with the value of 4.5, which can be seen that in the middle and late stages of creep, the right wall should be focused on.

(3) Fill completion 0, 1 year, the minimum value of the coefficient of safety site is the top of the arch, fill completion 10 years, the minimum value of the coefficient of safety site is the bottom of the right side wall. In 0 and 1 years after the completion of

filling, under the seismic effect, the safety coefficient of the arch top is the smallest in H1-2 condition, and in 10 years after the completion of filling, under the seismic effect, the safety coefficient of the side wall is the largest in H2-4 condition. Therefore, the structure has superior seismic performance in case H2-4.

## 6 Conclusion

The paper analyzes the perimeter soil pressure and lining safety performance of high-fill load-reducing open caves based on the equal load reduction rate and considering the timeliness of the fill, and the main conclusions are as follows:

(1) The average vertical dynamic soil pressure on the left side of the cave roof under seismic action for different time periods of fill completion is the static load 1.12~1.05~1.02 times of the earth pressure, and the moving earth pressure on the right side is 1.02~1.01~1 times of that on the left side; the average horizontal moving earth pressure on the left side (right side) of the hole is 0.63~0.88~1.03 times of the static loaded earth pressure (1.95~1.32~1.08 times). The change in dynamic soil pressure under earthquake was the largest in 0 years after the completion of the fill, and the change in dynamic soil pressure was the smallest in 10 years.

(2) In 0 years after the completion of the fill, the coefficient of safety from the right arch shoulder to the right wall decreased significantly under seismic action; In the year, the center of the superelevation arch has the largest decrease in the safety coefficient, and the left and right sides gradually tend to be symmetrical, but the location of the minimum value of the safety coefficient is still the top of the arch; in the year 10, the location of the minimum value of the safety coefficient is at the bottom of the right side wall. When seismic design is carried out in High-Filled Cuter Cover Tunnel, attention should be paid to the safety performance of the lining structure arch top and right side wall.

(3) The seismic performance under earthquake action at different time periods of filling completion can be analyzed from the point of view of soil pressure and safety coefficient on the roof and sides of the cave, and it is known that the seismic performance: virtual soil > mixed soil > EPS board. When openings are designed for load shedding seismic design, emphasis should be placed on the load shedding seismic performance of the voided soil.

## Acknowledgments

The authors would like to acknowledge the financial support provided by the National Science Foundation of China(51868041), the Basic Research Innovation Group Project of Gansu Province (21JR7RA347), the National Science Foundation of Gansu Province(22JR5RA338), the Key R & D Program Funding of Ningxia(2022BEG02056).

## References

1. Liu X K, LI S and WANG C D(2023). Finite difference based time-dependent study of soil arch morphology and structural response in high-fill reduced-load open caves[J/OL]. *Journal of Applied Mechanics*:1-10.
2. Zhang Y C, GAO F, LU G S, MA C and ZHAO Y(2018). Numerical simulation of high fill foundation settlement based on loess creep test[J]. *Science, Technology and Engineering*.
3. Ge M M, Li N,Zheng J G,Zhu C H and Ma X D(2015). Numerical study on post-work settlement law of loess high fill based on creep test[J]. *Journal of Xi'an University of Technology*.
4. Jia Y C (2021). Study on the long-term mechanical property evolution of high-fill open hole based on loess creep[D]. Lanzhou Jiaotong University.
5. Jia Y C, LI S and LI Z P et al(2020). Creep analysis of high fill loess open hole based on finite difference method[J]. *Journal of Railway Science and Engineering*, 17(08):2046-2054.
6. Gao Q, CHEN B G, WU S, YUAN S and SUN M Y(2023).Long-term force characteristics and load reduction effect of high-fill box culvert under load reduction condition of EPS plate[J/OL]. *Geotechnical Mechanics*, (07):1-11.
7. Wang F(2018). Safety evaluation of the second lining structure of a highway tunnel[J]. *Journal of Guangdong Transportation Vocational and Technical College*, 17(01):18-22.
8. Hu S J, WANG B(2014). Safety assessment of tunnel lining structure[J]. *Municipal Technology*, 32(06):71-73+78.
9. Ou X P, Guo H F and Yin H et al(2018). Stability analysis of tunnels based on rheological properties of wet subsiding loess[J]. *Journal of Wuhan University of Technology (Transportation Science and Engineering Edition)*, 42(03):435-439.
10. Nguyen D, Park D, Shamsher S, et al. Seismic vulnerability assessment of rectangular cut-and-cover subway tunnels[J]. *Tunnelling and Underground Space Technologyincorporating Trenchless Technology Research*,2019,86247-261.
11. Xian Z L, Chun T A, Lei H, et al. Seismic Dynamic Response Analysis of Mountain Tunnels with Seismic Reduction and Isolation Measures[J]. *KSCE Journal of Civil Engineering*,2022,27(1):109-121.
12. Yu Z G, LI S and HE C et al(2022). Study on soil arch morphology and dynamic response of lining structure of high-fill reduced-load open caves under earthquake[J]. *Earthquake Engineering and Engineering Vibration*, 42(05):186-195.
13. You ZG(2021). Study on soil pressure response and soil arch morphology of high-fill and reduced-load open caves under earthquake[D]. Lanzhou Jiaotong University.
14. Guo J, Wang M N and Tian S Z(2007). Seismic calculation and analysis of highway tunnel openings in high intensity seismic zone[J]. *Journal of Geotechnical Engineering*, (11):1733-1736.
15. Zhang X, Liu Y, Xiong F et al(2022). Seismic response analysis of rock tunnel portal section under oblique incidence of P-wave and SV-wave[J]. *Vibration and Shock*,41(24):278-286.
16. Yan Z X, Shi S, Jiang P et al(2013). Numerical analysis of dynamic response of tunnel under earthquake[J]. *Journal of Underground Space and Engineering*,9(05):1025-1029+1034.
17. Li S(2015). Research on vertical earth pressure characteristics and calculation method of unloading structure in open hole with high filling loess [D]. Lanzhou Jiaotong University.
18. Li S, Liu Y P, He C et al(2018). Unified calculation method of vertical earth pressure on the roof of trench-type high-fill loess open hole[J]. *China Railway Science*,39(05):1-7.



**Open Access** This chapter is licensed under the terms of the Creative Commons Attribution-NonCommercial 4.0 International License (<http://creativecommons.org/licenses/by-nc/4.0/>), which permits any noncommercial use, sharing, adaptation, distribution and reproduction in any medium or format, as long as you give appropriate credit to the original author(s) and the source, provide a link to the Creative Commons license and indicate if changes were made.

The images or other third party material in this chapter are included in the chapter's Creative Commons license, unless indicated otherwise in a credit line to the material. If material is not included in the chapter's Creative Commons license and your intended use is not permitted by statutory regulation or exceeds the permitted use, you will need to obtain permission directly from the copyright holder.

